Check for updates

NaHCO₃ as a carrier of CO₂ and its enhancement effect on mineralization during hydrothermal alteration of basalt

Sena Kikuchi, Jiajie Wang*, Otgonbayar Dandar, Masaoki Uno, Noriaki Watanabe, Nobuo Hirano and Noriyoshi Tsuchiya*

Department of Environmental Studies for Advanced Society, Graduate School of Environmental Studies, Tohoku University, Sendai, Japan

Reaction of carbon dioxide (CO_2) with minerals to generate stable carbonates, also known as CO_2 mineralization, has been regarded as one of the most promising methods for safe and permanent carbon storage. As a promising feedstock, basaltic rock has gained special interest, and elevating basalt carbonation efficiency with the reduction of negative environmental impact is the main challenge for CO_2 mineralization system development. Considering multiple potential positive effects of the CO_2 carrier, $NaHCO_3$, we conducted this study to experimentally evaluate the CO_2 storage efficiency during water-basalt-$NaHCO_3$ interactions under hydrothermal conditions at 200−300°C. The inclusion of $NaHCO_3$ was confirmed to drastically promote the alteration of basalt, especially at higher temperatures. As revealed by experiments conducted at the saturated vapor pressure of water, the carbon storage efficiency at 300°C reached 75 g/kg of basalt in 5 days, which was 12 times higher than that at 200°C. In such hydrothermal systems, basalt was carbonated to generate calcite ($CaCO_3$), where the Ca was mainly from plagioclase; Mg and Fe were incorporated into smectite, and Na in the saline system participated in the formation of Na silicates (i.e., analcime in the case of basalt). Due to the presence of additional Na in solution, all the released elements were consumed quickly with generation of secondary minerals in turn promoted basalt dissolution to release more Ca for CO_2 storage. This study illuminated the role of $NaHCO_3$ in basalt carbonation and provided technical backup to the design of advanced CO_2 mineralization systems.

KEYWORDS

carbon storage, basalt, sodium bicarbonate, hydrothermal system, calcite

1 Introduction

The urgent need to reduce the amount of carbon dioxide (CO_2) for creating a carbon neutral society has driven the development of various CO_2 capture, utilization, and storage (CCUS) techniques (Voigt et al., 2021). Among the CCUS techniques, mineralization of CO_2 to water-insoluble carbonates using Mg or Ca-rich rocks such as basalt (Goldberg et al., 2008; Okoko and Olaka, 2021), peridotite (Oelkers et al., 2008) and wollastonite (Wang et al., 2021) is a promising method for large-scale and long-term CO_2 storage with low risk of releasing stored CO_2 into the atmosphere (Zhao et al., 2015) and probably a relative acceptable cost (National Academies of Sciences, 2018; Kelemen et al., 2019). Basalt is one of the optimum

TABLE 1 Chemical compositions of basalt and anorthite determined using XRF.

Component	wt%	
	Basalt	Anorthite
SiO_2	47.59	42.70
TiO_2	1.64	n.d.
Al_2O_3	14.49	36.78
Fe_2O_3	12.57	0.31
MnO	0.19	n.d.
MgO	9.19	0.52
CaO	12.16	19.44
Na_2O	1.92	0.23
K_2O	0.15	n.d.
P_2O_5	0.11	n.d.
Total	100	99.98

Note: "n.d." indicates not determined.

rocks for CO_2 storage because of its chemical composition, abundant distribution and easy availability.

CarbFix Project in Iceland is an engineering example for large-scale CO_2 mineralization, where 95% of the dissolved CO_2 in freshwater is mineralized to carbonates in the basaltic groundwater setting which has a weakly alkaline pH and temperature of 20°C–50°C in 2 years (Alfredsson et al., 2013; Matter et al., 2016; Snæbjörnsdóttir et al., 2020). This successful application is inspiring other CO_2 mineralization projects around the world to be developed. However, it has been estimated that 22 tons of water is required to capture 1 ton of pure CO_2 for storage according to the operation in CarbFix (Snæbjörnsdóttir et al., 2020). To alleviate water shortage, recently, researchers suggested substituting freshwater with saline water (e.g., seawater) for long-term CO_2 storage (Voigt et al.,

2021), which makes the understanding of CO_2-saline water-basalt interactions even more important.

There have been many studies discussing the mineral alterations in CO_2-saturated NaCl saline systems at different pressures and temperatures (Ueda et al., 2021; Edem et al., 2022; Peter et al., 2022), however, many questions regarding reaction mechanisms are yet to be answered. NaCl is the most abundant salt component in saline aquifers, while also contains minor Ca^{2+}, Mg^{2+}, HCO_3^- and SO_4^{2-}, etc., Due to the high ionic strength in the CO_2-saturated NaCl saline system, the dissolution of silicates minerals to release Ca and Mg ions (Gudbrandsson et al., 2011; Wang et al., 2019; Bratcher et al., 2021), which subsequently react with CO_2 to generate carbonate minerals, can be enhanced (Wang and Giammar 2013; Marieni et al., 2020). However, debates on the independent effects of NaCl and dissolved CO_2 species (e.g., $NaHCO_3$ in saline water) on CO_2 mineralization are still ongoing. Although $NaHCO_3$ is a relatively minor component in saline water, it is the main carrier for CO_2 and can directly participate in CO_2 mineralization. Gadikota et al. (Gadikota et al., 2014) proposed that $NaHCO_3$ may be a more crucial factor in olivine carbonation promotion than NaCl because the carbonation process significantly influences the surface area and particle size of olivine, which induces further carbonation. Our previous research on hydrothermal olivine alteration also found enhanced olivine dissolution and carbonation in CO_2-rich while Cl-free environments (Wang et al., 2019a). However, since the mineral composition of basalt is relatively complex, whether $NaHCO_3$ has a potentially positive role in basaltic rock carbonation has yet to be confirmed.

Another important but less studied aspect of basalt carbonation is related to the carbonate formations under high temperature conditions. Although higher temperatures are favorable for mineral dissolution (Casey and Sposito, 1992; Wang et al., 2019b), the suggested temperatures for basalt carbonation were generally ≤200°C due to the competitive hydrothermal alteration reactions. Among the previous studies, Rosenbauer et al. (Rosenbauer et al., 2012) conducted basalt carbonation experiments using a CO_2-rich NaCl brine at 50°C–200°C; however, the maximum carbonation rate occurred at 100°C with
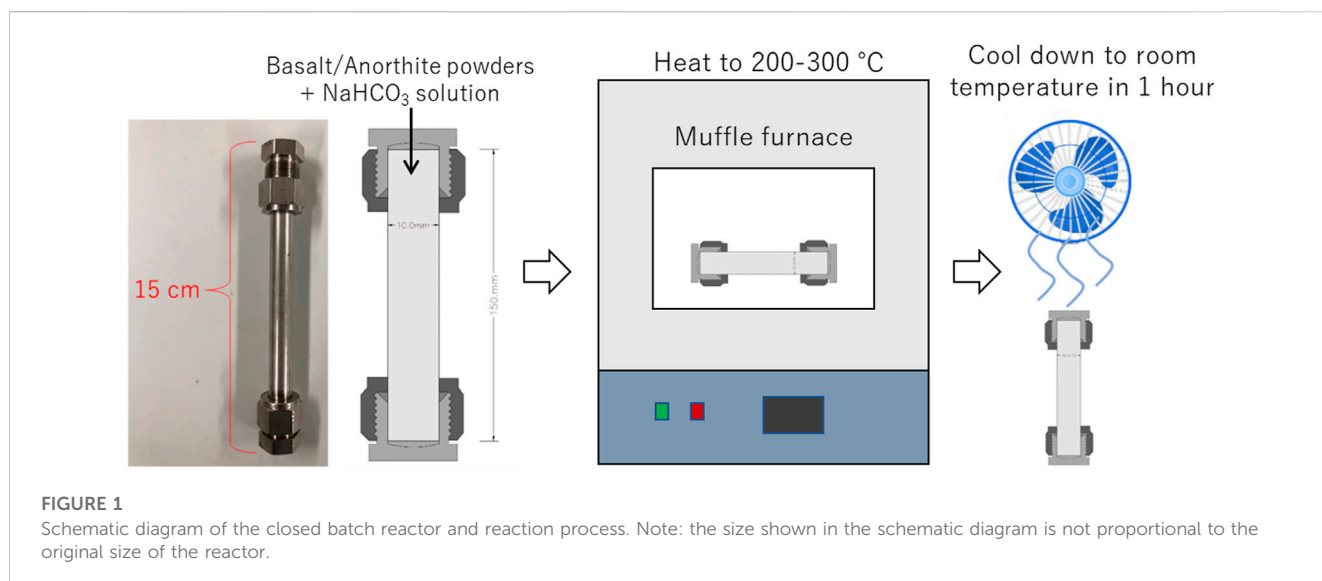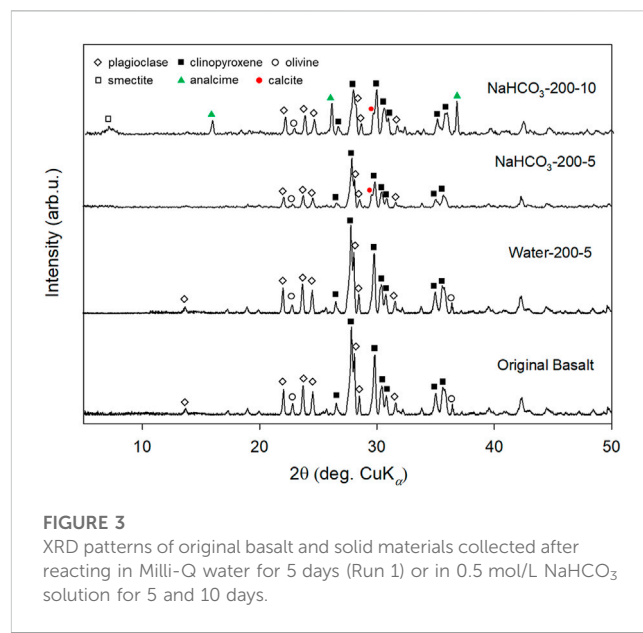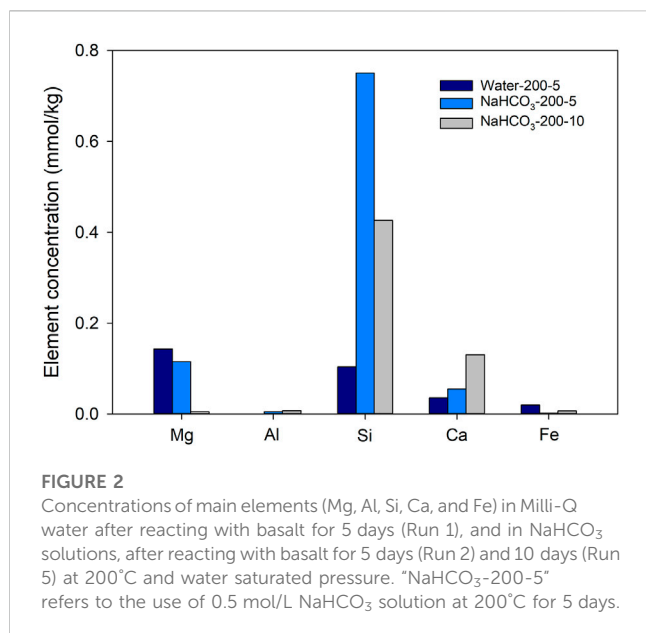

FIGURE 1
Schematic diagram of the closed batch reactor and reaction process. Note: the size shown in the schematic diagram is not proportional to the original size of the reactor.

TABLE 2 Experimental conditions for basalt carbonation.

Exp	Rock	Solution[a]	T (°C)	Duration (days)	pH$_0$[b]	pH$_{in-situ}$[b]	pH$_t$[b]	Secondary minerals
1	basalt	Milli-Q	200	5	7.9	7.5	7.9	—
2	basalt	NaHCO$_3$	200	5	8.2	8.3	8.5	Calcite
2b	—	NaHCO$_3$	200	5	8.2	8.3	8.2	—
3	basalt	NaHCO$_3$	230	5	8.2	8.4	8.4	Calcite, Analcime, Smectite
3b	—	NaHCO$_3$	230	5	8.2	8.4	8.2	—
4	basalt	NaHCO$_3$	300	5	8.2	9.0	8.4	Calcite, Analcime, Smectite
4b	—	NaHCO$_3$	300	5	8.2	9.0	8.2	—
5	basalt	NaHCO$_3$	200	10	8.2	8.3	8.3	Calcite, Analcime, Smectite
6	Anorthite	Milli-Q	300	5	7.2	7.5	8.1	—
7	Anorthite	NaHCO$_3$	300	5	8.3	9.0	8.9	Calcite, Cancrinite

[a]Concentration of NaHCO$_3$ was 0.5 mol/L for all experiments.
[b]pH$_0$ and pH$_t$ respectively refer to the pH measured before and after experiments at room temperatures, while pH$_{in-situ}$ refers to the pH at the experimental temperature, calculated using SOLVEQ.

FIGURE 2
Concentrations of main elements (Mg, Al, Si, Ca, and Fe) in Milli-Q water after reacting with basalt for 5 days (Run 1), and in NaHCO$_3$ solutions, after reacting with basalt for 5 days (Run 2) and 10 days (Run 5) at 200°C and water saturated pressure. "NaHCO$_3$-200-5" refers to the use of 0.5 mol/L NaHCO$_3$ solution at 200°C for 5 days.

FIGURE 3
XRD patterns of original basalt and solid materials collected after reacting in Milli-Q water for 5 days (Run 1) or in 0.5 mol/L NaHCO$_3$ solution for 5 and 10 days.

ferroan magnesite [(Mg, Fe)CO$_3$] as the main carbonation product. On the other hand, Wolff-Boenisch and Galeczka (Wolff-Boenisch and Galeczka, 2018) reported the carbonation products were calcite and Ca/Mg-carbonates at 90°C in synthetic seawater. Due to these mutually inconsistent results, more studies are needed to establish the mechanism of basalt carbonation especially at high temperatures.

This paper aims to address the above research vacancy by evaluating CO$_2$ storage efficiency and revealing the independent effects of NaHCO$_3$ during basalt alteration in hydrothermal systems which is Cl-free through a series of batch experiments conducted at 200°C–300°C. Basaltic rocks obtained from Iceland were used for reaction. This study experimentally verified the hypothesis using a CO$_2$-rich hydrothermal environment to promote CO$_2$ storage through basalt carbonation and clarified how Na joins water-basalt-CO$_2$ interactions. The study results are expected to quantify the CO$_2$ mineralization potential of using such systems and to provide technical backup for the development of CO$_2$ mineralization systems using basalt or other rocks.

2 Materials and methods

2.1 Materials

The basaltic rock used in this study was obtained from Iceland (MORB), which is one of the most widely studied areas for CO$_2$ storage, the reactivity of these basaltic rocks has been confirmed by other studies (Matter et al., 2016; Snæbjörnsdóttir and Gislason, 2016; Snæbjörnsdóttir et al., 2020) and is thus easier for comparison. Its
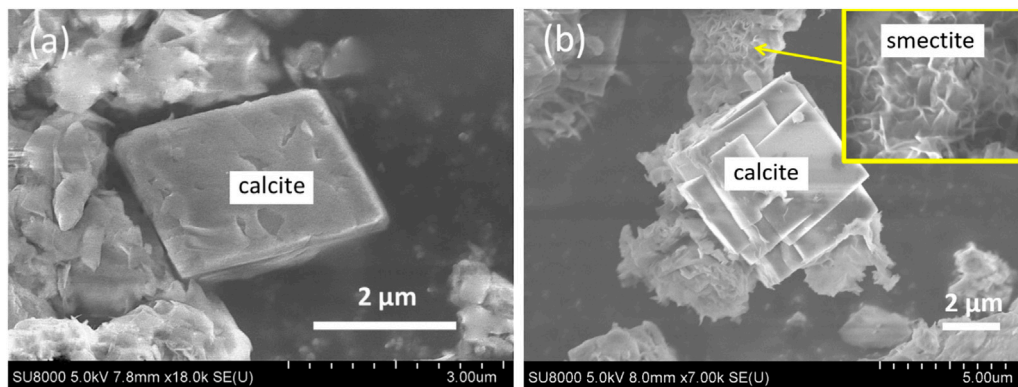
FIGURE 4
SEM images of solid samples collected after reacting in 0.5 mol/L NaHCO$_3$ solution for **(A)** 5 days and **(B)** 10 days.

main mineral compositions were plagioclase (Ca$_{0.7}$Na$_{0.3}$Al$_{1.7}$Si$_{2.3}$O$_8$), clinopyroxene (Ca$_{0.8}$Mg$_{0.7}$Fe$_{0.5}$Si$_2$O$_6$), olivine (Mg$_{1.6}$Fe$_{0.4}$SiO$_4$), glass, Fe-Ti oxides, and Cr oxide, determined using an electron probe microanalyzer (EPMA, JEOL JXA-8200) at Tohoku University. The average chemical composition of the rock is shown in Table 1, quantified *via* X-ray fluorescence (XRF, Rigaku, ZSX Primus IV) measurement. The basaltic rock was ground and sieved to obtain the <63 μm-sized fraction for experiments. Anorthite (CaAl$_2$Si$_2$O$_8$), an endmember of plagioclase solid solutions, with only a small amount of Na, was also used for experiments in this study to reproduce the albitization process of plagioclase observed in experiments using basalt as well as to quantify the effects of Na in solution on promoting mineral alteration. The anorthite used was obtained from Hokkaido, Japan, with the compositions shown in Table 1. The particles selected for the experiments were relatively coarse, with sizes ranging from 63–125 μm. Sodium bicarbonate (NaHCO$_3$) purchased from Kanto Chemical (Japan) was used to create Na-rich systems and used as the CO$_2$ source for storage.

2.2 Experimental design and measurement

A closed batch reactor with a length of 150 mm, diameter of 10 mm, and internal volume of 13 mL was used in this study for hydrothermal experiments (Figure 1). The reactor body was made of SUS316, with the main compositions of Fe, Ni, Cr, as well as few Mo, Si, Mn, C, P, and S. The reactor was easy to operate and could be put in a muffle furnace (Yamato, FP31) for hydrothermal reactions. The tolerated temperature of the reactor was 400°C and the pressure was 10 MPa. For each experiment, 8 mL solution was injected into the reactor with the filling ratio of around 62%.

The experimental conditions for basalt alteration are shown in Table 2. In Runs 2, 3, 4, and 5, 0.5 mol/L NaHCO$_3$ solution was prepared for basalt alteration, this concentration has been proved to be effective in promoting the carbonation of olivine in our previous study (Wang et al., 2019a). Run 1 used Milli-Q water, the pH of which was also adjusted to weak alkaline, similar to the value of NaHCO$_3$ solution using NaOH solution. Runs 1 and 2 were conducted to verify the positive effects of NaHCO$_3$ on basalt
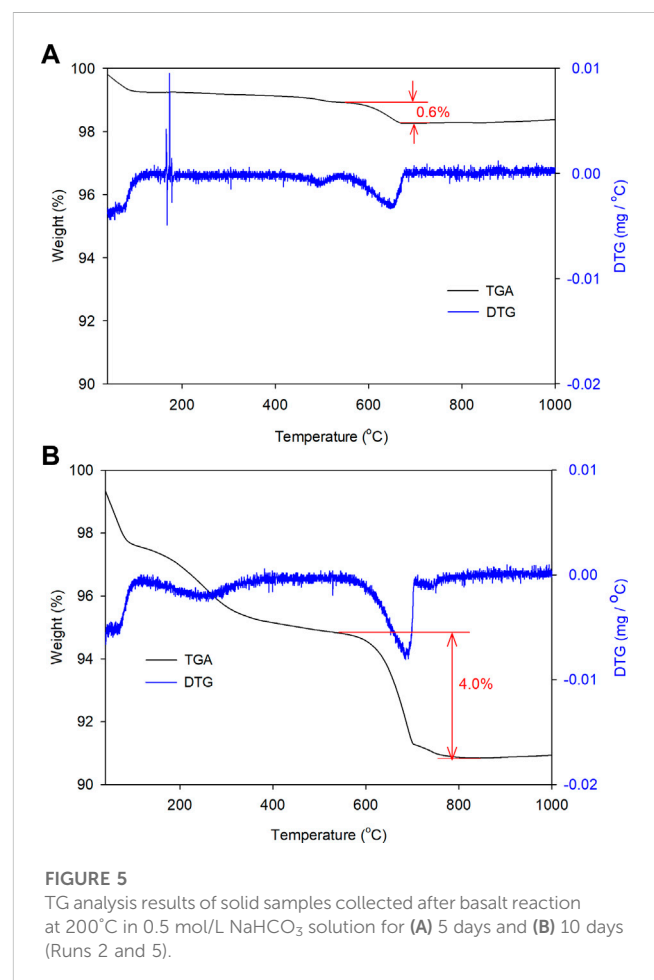

FIGURE 5
TG analysis results of solid samples collected after basalt reaction at 200°C in 0.5 mol/L NaHCO$_3$ solution for **(A)** 5 days and **(B)** 10 days (Runs 2 and 5).

alteration. Runs 2, 3, and 4 were tested to study the effects of reaction temperature while Run 5 was conducted to compare with Run 2 to illustrate the effect of reaction duration. In all the above experiments, 0.3 g basalt powder was added into the reactor tube, followed by addition of 6 mL of 0.5 mol/L NaHCO$_3$ solution prepared using Milli-Q water. The reactor was sealed and gently

TABLE 3 Saturation indexes (SI) of minerals in the NaHCO₃ experiments.

Expª	Duration (day)	T (°C)	Saturation index			
			Calcite	Anorthite	Diopside	Analcime
2	5	200	1.3	−5.5	2.6	−2.2
3	5	230	2.2	−2.5	4.3	−0.9
4	5	300	2.3	−1.7	6.1	−1.4
5	10	200	1.6	−5.1	0.5	−2.4

ªNumbers of Exp. Are consistent with those shown in Table 2.

FIGURE 6
Concentrations of Mg, Al, Si, Ca, and Fe in NaHCO₃ solutions after reacting with basalt at 200°C, 230°C, and 300°C for 5 days (Runs 2–4).

FIGURE 7
XRD patterns of solid samples collected after reacting basalt in 0.5 mol/L NaHCO₃ solution at 200°C, 230°C, and 300°C for 5 days (Runs 2–4).
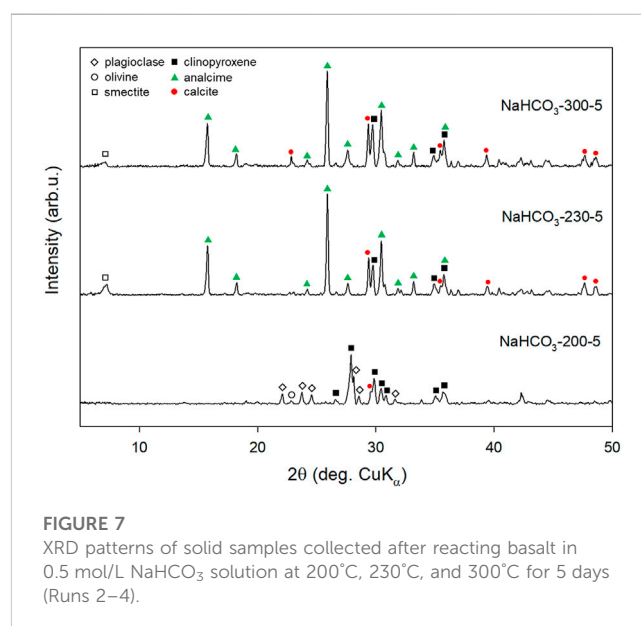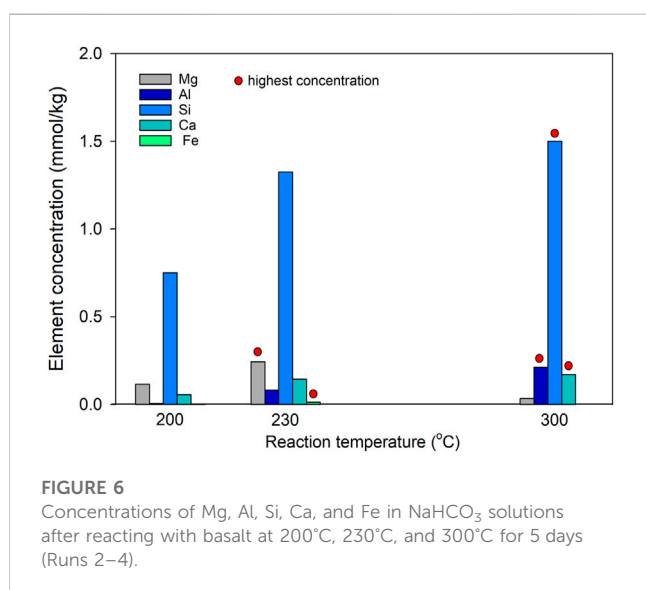
shaken to mix the solid and fluid, following which it was vertically put into a muffle furnace, whose internal temperature was assumed to quickly increased to a desired value (200°C–300°C); meanwhile, the pressure was increased to water-saturated pressure for reactions (<8.5 MPa). After keeping the reactor at a constant temperature for 5–10 days for reaction, it was taken out from the muffle furnace and cooled to room temperature (~20°C) within 1 h using a fan. The reaction rate is considered slow at ambient temperatures; thus the reaction is assumed to have stopped. The reactor with solution inside was weighed before and after reaction to ensure that no liquid has leaked out of the reactor and that the reactor was highly gas tight. The solid and liquid samples were then separated for analysis. To eliminate if elements have been released from the autoclaves or not, blank experiments (remarked as 2b, 3b and 4b in Table 2) without rocks were also conducted at each temperature.

All liquid samples taken after the reactions were analyzed *via* inductively coupled plasma-optical emission spectrometry (ICP-OES; Agilent 5100) to quantify the target elements (e.g., Mg, Al, Si, Ca, Fe). The concentration of Na was not analyzed in this study due to the initial inclusion of a high concentration of NaHCO₃. Each fluid sample was measured for three times, showing good reproducibility within a margin of error of 3%. The pH of the suspension was measured at room temperature (around 20°C). The solid samples were washed with Milli-Q water and dried in an oven

with a temperature of 60°C for 24 h before mineral composition measurement using X-ray diffraction (XRD; Multiflex, Rigaku, Japan) with Cu Kα radiation ($\lambda = 1.54$ Å) operated at 40 kV and 20 mA and with a 2θ step size of 0.02° from 5° to 50°. The surface morphologies of minerals were observed using scanning electron microscopy (SEM; SU-8000, Hitachi, Japan) equipped with energy dispersive spectroscopy. Thermogravimetric (TG) analyses of all reacted minerals were performed using a thermogravimetry (Thermo plus EVO TG 8120, Rigaku, Japan). The temperature was increased from room temperature to 1000°C at a rate of 10°C/min. The carbonate fraction was determined from the weight loss due to CO_2 release in a specific temperature range, for instance, calcite was decomposed to release CO_2 at around 500–780°C (Wang et al., 2019).

3 Results and discussion

3.1 Effects of NaHCO₃ as a function of reaction duration

The solution pH showed no obvious change in basalt-Milli-Q water experiment and in blank experiments without basalt, while it slightly increased after reaction of basalt in NaHCO₃ solution
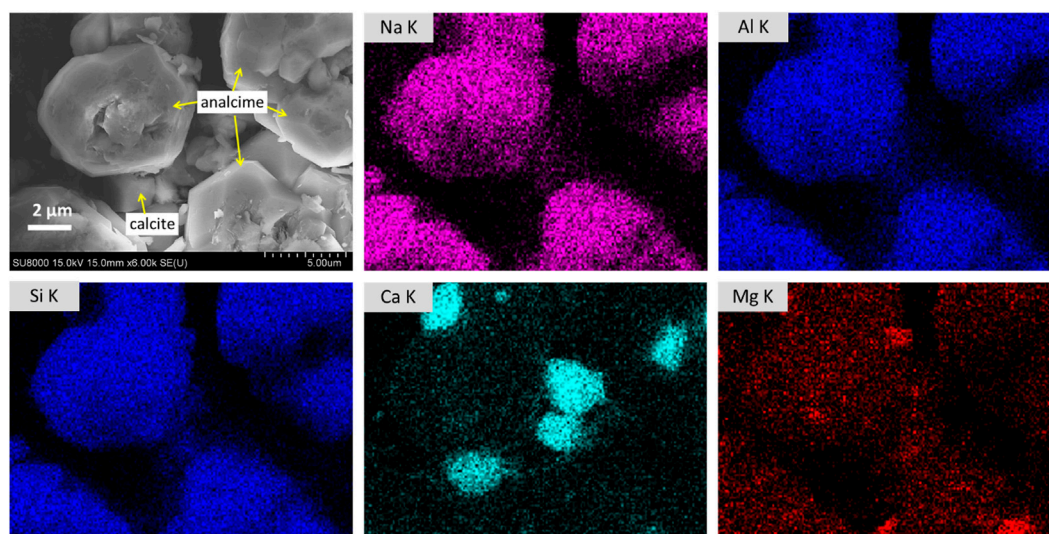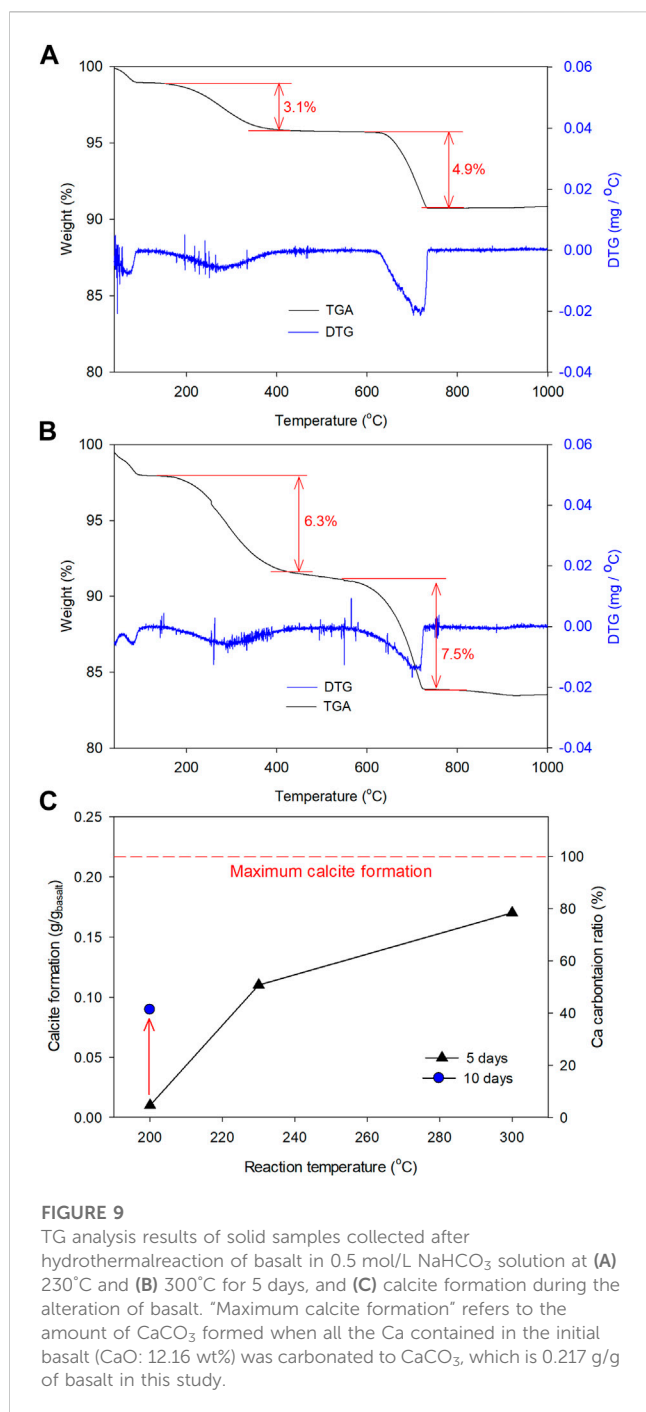
FIGURE 8
SEM images and EDS measurement of analcime and calcite in solid samples collected after reacting basalt in NaHCO$_3$ solution at 300°C for 5 days (Run 4). Deltoidal icositetrahedrons with the main chemical composition of Na, Al, and Si were considered as analcime whereas small Ca-rich particles between analcime were considered as calcite.

(Table 2). This change was considered a result of silicate dissolution (Zhi and Ying, 1993), or the CO$_2$ degassing/dissolution process during heating and cooling the autoclave (Shibuya et al., 2013). Solutions obtained from blank experiments (without basalt) contained only a few dissolved Fe, with a concentration ≤0.004 mmol/kg, while other elements are lower than the detection limitation, suggesting influence from the autoclaves is negligible. The concentrations of leached elements in black experiments with basalt addition are shown in Figure 2. Obvious increases in Si concentration were observed in experiments with NaHCO$_3$ solution (Runs 2 and 5). Although elemental concentrations are not always consistent with the extent of dissolution, especially at hydrothermal conditions due to generation of secondary minerals, such drastic increase in Si concentration can be a result of the enhanced dissolution of basalt with the use of Na and CO$_2$-rich water. In 5 days, the Si concentration in NaHCO$_3$ solution was much higher than that in water. This high Si concentration then decreased with the reaction duration increased from 5 to 10 days, which was attributed to the generation of secondary silicate minerals. The concentrations of Mg in NaHCO$_3$ experiment also decreased as the reaction duration increased from 5 to 10 days, suggesting the formation of Mg-bearing secondary minerals.

The XRD patterns of original basalt and solid materials collected after experiments are shown in Figure 3. The XRD pattern of solid sample did not show any obvious change after reaction with Milli-Q water for 5 days, indicating that the secondary mineral was not generated, or the generated amount was too less to be detected. However, the peaks of plagioclase, clinopyroxene, and olivine were smaller after reacting with 0.5 mol/L NaHCO$_3$ solution, than those of original basalt, such as the obvious diminishing peak of plagioclase at 13.5°. The preferred dissolution of plagioclase over clinopyroxene from basalt was consistent with the result of Nesbitt and Wilson (1992) (Nesbitt and Wilson, 1992). Calcite is the main product of basalt carbonation, as evidenced by the characteristic calcite peak at 29.6° (2θ, CuKα) (Wang et al., 2021) after reaction of basalt in NaHCO$_3$ solution, and the calcite peak showed higher intensity when the reaction time increased from 5 to 10 days, suggesting an increase in calcite concentration in the reacted sample. Meanwhile, peaks of analcime (e.g., 15.8°, 26.0°), a Na-Al silicate with the general chemical formula of NaAlSi$_2$O$_6$·H$_2$O, and smectite (in the range of 6.3°–8.0°), a clay mineral contains Mg, Fe, Si, as well as Al (Yamashita et al., 2019), were also detected. This finding was also evidenced by SEM images, as shown in Figures 4A, B. Rhombohedron calcite was observed in both experiments using NaHCO$_3$ solution, but an increase in calcite particle size from 2 μm to >4 μm was observed when the reaction time increased from 5 to 10 days. Smectite with honeycomb texture was only observed on the surface of basalt after reaction in NaHCO$_3$ solution for 10 days (Figure 4B). However, analcime was not found during SEM observations even though XRD suggested its generation, which might be covered by smectite. The generation of analcime and smectite during reaction between 5 and 10 days was consistent with the ICP-OES result, i.e., the decrease in Mg and Si concentrations.

Calcite in the reacted samples obtained from Runs 2 and 5 was quantified via TG analysis and the first derivative curves (Figure 5). The weight loss at 500–780°C was assigned to the decomposition of Ca carbonates (loss of CO$_2$), based on previous studies (Wang et al., 2022). Therefore, weight losses of 0.6% and 4.0% for solid samples collected on Day 5 and 10 of experiments with NaHCO$_3$ indicated that the calcite mass fractions reached 1.4 wt% and 9.1 wt%, respectively. On ignoring the changes in the total weight of solids during reactions, calcite formation in the later 5 days was 5.5 times higher than that formed during the initial 5 days. This kind of enhancement was unexpected because rocks generally dissolve faster in the initial stage due to the presence of finer rock particles and more fresh surface area for dissolution. The saturation index (SI) of

FIGURE 9
TG analysis results of solid samples collected after hydrothermalreaction of basalt in 0.5 mol/L NaHCO₃ solution at **(A)** 230°C and **(B)** 300°C for 5 days, and **(C)** calcite formation during the alteration of basalt. "Maximum calcite formation" refers to the amount of $CaCO_3$ formed when all the Ca contained in the initial basalt (CaO: 12.16 wt%) was carbonated to $CaCO_3$, which is 0.217 g/g of basalt in this study.

calcite was then calculated using SOLVEQ based on the composition of fluid obtained after each experiment, the results are shown in Table 3. In the 10-day experiment at 200°C, SI of calcite (1.6) is slightly increased than that of 5-day experiment at 200°C (1.3), which is consistent with the experimental observation. It should also be noted that for Day 10 sample, an additional weight loss was observed at around 110–380°C, which might be attributed to the dehydration of analcime and smectite, as suggested by Liu et al. (2019); Frost and Ruan (2000). However, weight loss at 400–500°C, which usually represents the dehydroxylation of smectite (Frost and

Ruan, 2000), was little, suggesting smectite fraction was minor in the reacted samples while most secondary silicate was analcime. Therefore, the acceleration of carbonation at the latter stage of the 10-day experiment might be related to both a higher SI of calcite and the formation of analcime with the change in fluid chemistry. This process consumed the dissolved elements and triggered further dissolution of basalt.

3.2 Effects of NaHCO₃ as a function of temperature

Basalt was reacted in 0.5 mol/L NaHCO₃ solution at 200°C, 230°C and 300°C, respectively, for 5 days to clarify the effects of temperature on CO_2 storage. The chemistry measurement of fluids obtained after each experiment indicated that a higher temperature might favor basalt dissolution, as evidenced by the high concentrations of Si, Al, and Ca at higher reaction temperatures (Figure 6). This kind of enhanced dissolution was particularly notable when the temperature was ≥230°C. However, the same result was not observed in Mg and Fe concentrations, which, on the contrary, decreased when the reaction temperature increased from 230°C to 300°C, which might be related to the promoted generation of Mg and Fe bearing secondary minerals such as smectite at a higher temperature.

XRD measurement of the reacted solids collected after reacting in NaHCO₃ solution at 230°C and 300°C for 5 days showed that in almost all characteristic peaks of plagioclase and olivine, the original compositions of basalt were diminished whereas clinopyroxene peaks were relatively stronger due to the consumption of other minerals (Figure 7). This observation suggested that during basalt dissolution in hydrothermal CO_2-rich saline systems, the dissolution of plagioclase and olivine was relatively faster while clinopyroxene may be the last one to be dissolved. It should be noted that this kind of peak diminishment does not mean that all minerals have been dissolved or reacted because mineral alteration occurs from the surface and the penetration depth of XRD measurement is limited to dozens of microns. Meanwhile, strong analcime and calcite peaks were observed in experiments conducted at 230°C and 300°C. According to SEM observation, analcime crystals with typical deltoidal icositetrahedron habit grew up to 6 μm in size (Figure 8) at the reaction temperature of 300°C. Among analcime particles, smaller calcite particles were observed as compared to analcime particles. The SI of calcite increases from 1.3 to 2.3 with the increase of reaction temperature from 200°C to 300°C, which is consistent with the experimental observations that more calcite was generated at a higher temperature. In this study, although basalt was dissolved to simultaneously release Mg, Ca, and Fe, the only carbonate generated is calcite [Ca carbonation with few Mg, Ca/(Ca + Mg) = 0.95] in all experiments using NaHCO₃ solutions (Runs 2–5). At such high temperature, very small amount of Mg has contributed to the formation of carbonates.

As expected from the fluid chemistry measurement results and confirmation by the TG analysis, at a higher temperature, more calcite was generated. The weight loss at 500–780°C for samples reacted in NaHCO₃ solutions at 230°C and 300°C were 4.9% and
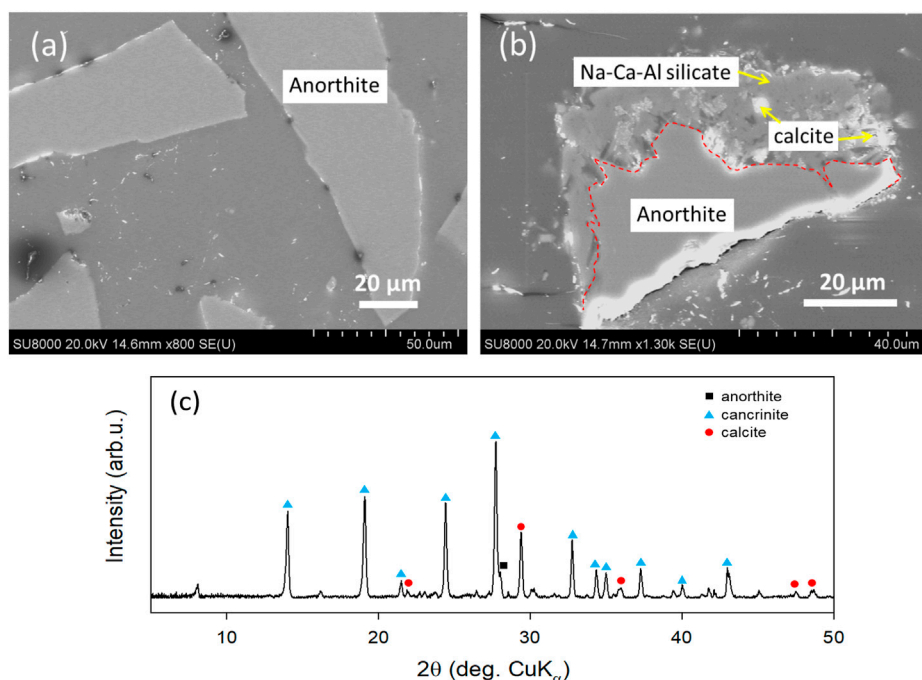
FIGURE 10
SEM images and XRD patterns of solid samples obtained after reaction of anorthite in **(A)** Milli-Q water and **(B,C)** 0.5 mol/L NaHCO$_3$ solution at 300°C for 5 days. A clear boundary between reacted and unreacted anorthite is marked with a red dashed line.
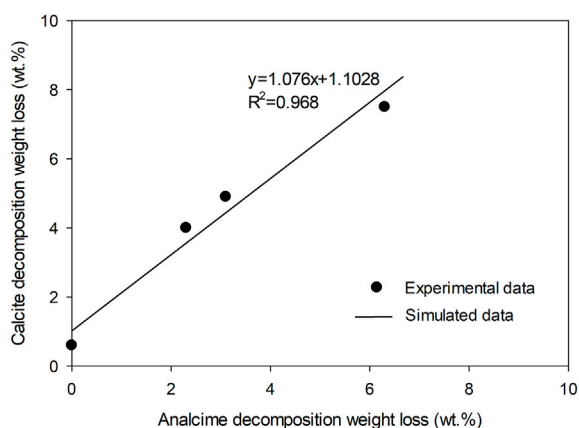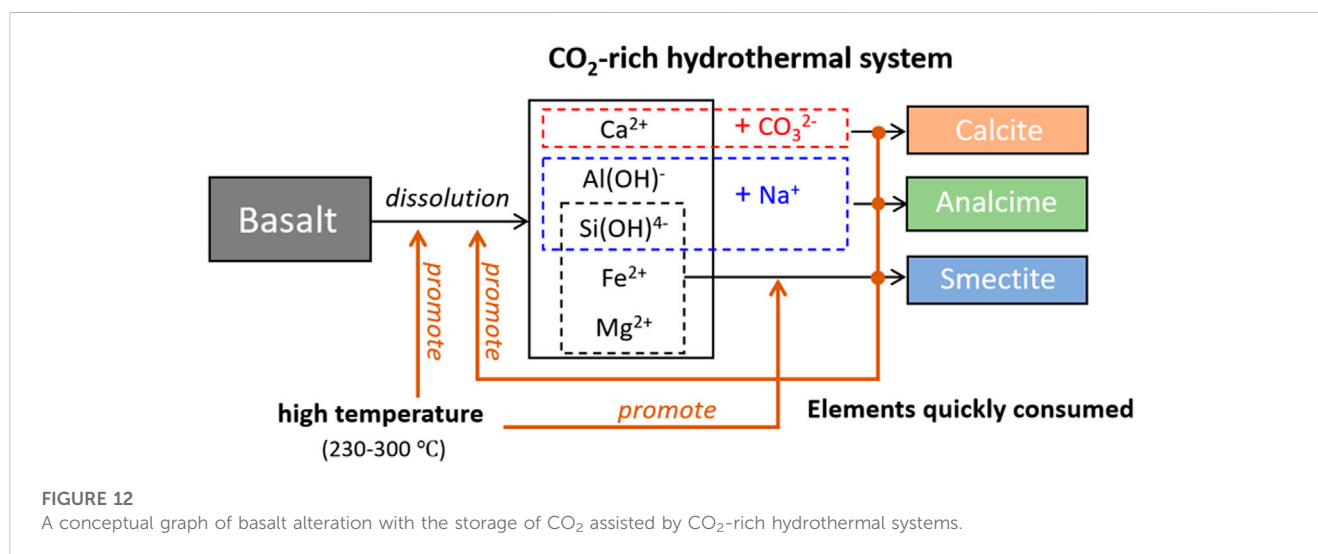

FIGURE 11
A potential relationship between calcite and analcime generation indicated by the weight loss due to calcite and analcime decomposition during TG measurement of the solid samples collected after reaction in NaHCO$_3$ solution at 200°C−300°C for 5−10 days.

7.5% (Figure 9), respectively, suggesting the calcite fractions of 11.1 wt% and 17.0 wt%, which were 7.9 and 12.1 times higher than that generated at 200°C, respectively. If the weight changes during basalt alteration were ignored, the approximate calcite formation from basalt carbonation under different conditions was calculated and summarized in Figure 9C. In this study, the initial basalt contained 12.16 wt% CaO, which means if all Ca carbonated,

CaCO$_3$ formation efficiency was 0.217 g/g of basalt. Further, reaction with NaHCO$_3$ solution at 300°C suggested that approximately 79% of Ca in basalt was carbonated to form calcite in 5 days and this ratio could be elevated if the reaction time was extended. The CO$_2$ storage efficiency at 300°C was 75 g/kg of basalt in 5 days. With the increase in calcite generation, analcime generation also enhanced, as indicated by a larger weight loss at 110–380°C, which indicates a positive correlation between albitization and calcium carbonate formation process.

3.3 Albitization and calcium carbonate formation reproduction using anorthite

To reproduce the albitization process which has been observed in basalt experiments and to have a better observation of how NaHCO$_3$ promote mineral dissolution and carbonation, anorthite (CaAl$_2$Si$_2$O$_8$) with negligible amount of Na, was reacted in both Milli-Q water and 0.5 mol/L NaHCO$_3$ solution at 300°C for 5 days. Thin sections of the solid samples collected after reaction were prepared and observed *via* SEM. In water system, the surface of anorthite (edge of particles shown in Figure 10A) was rarely altered and no secondary minerals were found whereas in the Na and CO$_2$-rich system (i.e., NaHCO$_3$ solution), nearly half of the anorthite was reacted, as revealed by a clear boundary between reacted and unreacted anorthite (Figure 10B). In the reacted region, EDS measurement suggested that the compositions of the base were mainly Na, Ca, Al, and Si while calcite particles distributed along the base. Results of XRD analysis of the reacted anorthite also suggested the generation of calcite and cancrinite in the experiment with NaHCO$_3$ solution (Figure 10C).
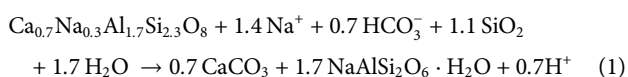
FIGURE 12
A conceptual graph of basalt alteration with the storage of CO_2 assisted by CO_2-rich hydrothermal systems.

Cancrinite is a complex carbonate and silicate with a general composition of $Na_6Ca_2[(CO_3)_2|Al_6Si_6O_{24}]\cdot 2H_2O$ (Seo et al., 2018). However, also due to the formation of cancrinite, the carbonation efficiency could not be determined according to TG analysis, because the weight losses due to cancrinite and calcite decompositions were overlapped (Hassan et al., 2006).

4 Discussion

Due to the urgent need of decreasing atmospheric CO_2 concentration, mineralization of CO_2 into carbonates using rocks, especially the abundant and widely distributed one, basalt, has raised a lot of interest. This study provided fundamental insight into the process of basalt carbonation in a CO_2-rich hydrothermal system and experimentally confirmed the enhancement of basalt carbonation with generation of more calcite in such system with a higher temperature.

A positive relationship between calcite and secondary silicate minerals such as analcime and smectite formation was revealed by the experiments. According to TG analysis, weight loss occurred at 500–780°C and 110–380°C, which has been assigned to the decomposition of calcite and analcime, respectively, indicating a good linear relationship with coefficient factor R^2 up to 0.968 (Figure 11). Assuming that calcite and analcime fractions are directly proportional to their weight losses during TG measurement, their generations show good linear relationship. In 200°C $NaHCO_3$ solution, analcime was not generated in 5 days, possibly because the concentration of Si was not high enough, which increased with the reaction time and finally triggered analcime formation after 5 days reaction. Such kind of secondary mineral formation in turn promoted more basalt to be dissolved and generated more calcite. The formation of calcite from plagioclase may present as follows (Eq. 1), where the hydrothermal fluids and pyroxenes provided additional Na^+ and Si sources.

$$Ca_{0.7}Na_{0.3}Al_{1.7}Si_{2.3}O_8 + 1.4\,Na^+ + 0.7\,HCO_3^- + 1.1\,SiO_2$$
$$+ 1.7\,H_2O \rightarrow 0.7\,CaCO_3 + 1.7\,NaAlSi_2O_6 \cdot H_2O + 0.7H^+ \quad (1)$$

This study suggested that $NaHCO_3$ in hydrothermal systems plays a crucial role in enhancing CO_2 storage as well as promoting the generation of secondary silicates such as analcime during the alteration of basalt (illustrated in Figure 12). The use of such Cl-free and weaker acid fluid may be helpful to minimize the corrosion of CO_2 injection tubes during the engineering process of CO_2 mineralization. However, although this study suggested hydrothermal conditions for basalt carbonation, operation management in such high-temperature reservoirs is usually difficult and CO_2 storage efficiencies change with the unstable geothermal system. Instead, using the chemical engineering process and industrial waste heat for high-temperature basalt carbonation will be more controllable; at the same time, it contributes to the efficient utilization of basaltic slags. According to the experiments conducted in this study, 0.17 kg calcite could be formed during the alteration of 1 kg basalt in 20 L $NaHCO_3$ at 300°C. If assuming the initial system temperature is 25°C, 9.72×10^{-2} GWh energy is required to heat the system to 300°C for storing 1 ton of CO_2; and this energy can be supplied by waste heat produced in non-metallic mineral, chemical and petrochemical, iron and steel industry sectors (Bianchi et al., 2019). Another way of applying this finding is in the CO_2 plume geothermal power generation process, during which basalt is one of target rocks and some amount of CO_2 may be stored as minerals at the edges of the reservoir. The use of $NaHCO_3$ hydrothermal fluid may contribute to keeping the bulk of CO_2 inside the geothermal reservoir. Based on these findings, further studies should focus on developing a better understanding of the dissolution behaviors of basalt blocks in Na-rich hydrothermal systems and changes in subsequent rock properties as a function of reaction time with a view to expand the efficient utilization of basalt reservoirs for CO_2 capture and storage. Moreover, the effect of basalt properties on CO_2 storage efficiency should also be clarified.

5 Conclusion

The present study experimentally quantified the effects of $NaHCO_3$ on basalt carbonation at 200–300°C in Cl-free environments. The

presence of NaHCO$_3$ was confirmed to drastically promote the alteration of basalt with accelerated CO$_2$ storage, especially at higher temperatures. The CO$_2$ storage efficiency at 300°C reached 75 g/kg of basalt in 5 days, which was 12.1 times higher than that at 200°C. In such hydrothermal systems, basalt was altered to generate mainly calcite, analcime, and smectite. Further, the dominant element for CO$_2$ storage was Ca mainly from plagioclase, while released Mg and Fe were converted to clay minerals such as smectite. Na in the system participated in the formation of Na silicates such as analcime in the case of basalt. In this way, the main elements released during basalt dissolution were quickly consumed in secondary mineral generations, which in turn promoted basalt dissolution to release more Ca and CO$_2$ storage. Fundamental effects of adding NaHCO$_3$ for basalt alteration have been considered in this paper, however, detailed chemical mechanisms should be investigated as further studies.

Data availability statement

The raw data supporting the conclusions of this article will be made available by the authors, without undue reservation.

Author contributions

SK: conceptualization, methodology, data curation, formal analysis, writing-original draft. JW, NW and NT: conceptualization, methodology, investigation, funding acquisition, project administration, resources, writing-original draft and writing-reviewing and editing. OD, MU and NH: investigation, methodology, software, writing-reviewing and editing. All authors contributed to the article and approved the submitted version.

Conflict of interest

The authors declare that the research was conducted in the absence of any commercial or financial relationships that could be construed as a potential conflict of interest.

Publisher's note

All claims expressed in this article are solely those of the authors and do not necessarily represent those of their affiliated organizations, or those of the publisher, the editors and the reviewers. Any product that may be evaluated in this article, or claim that may be made by its manufacturer, is not guaranteed or endorsed by the publisher.

References

Alfredsson, H. A., Oelkers, E. H., Hardarsson, B. S., Franzson, H., Gunnlaugsson, E., and Gislason, S. R. (2013). The geology and water chemistry of the Hellisheidi, SW-Iceland carbon storage site. *Int. J. Greenh. Gas. Control* 12, 399–418. doi:10.1016/j.ijggc.2012.11.019

Bianchi, G., Panayiotou, G. P., Aresti, L., Kalogirou, S. A., Florides, G. A., Tsamos, K., et al. (2019). Estimating the waste heat recovery in the European Union Industry. *Energ. Ecol. Environ.* 4, 211–221. doi:10.1007/s40974-019-00132-7

Bratcher, J. C., Kaszuba, J. P., Herz-Thyhsen, R. J., and Dewey, J. C. (2021). Ionic strength and pH effects on water–rock interaction in an unconventional siliceous reservoir: On the use of formation water in hydraulic fracturing. *Energy fuels.* 35, 18414–18429. doi:10.1021/acs.energyfuels.1c02322

Casey, W. H., and Sposito, G. (1992). On the temperature dependence of mineral dissolution rates. *Geochimica Cosmochimica Acta* 56, 3825–3830. doi:10.1016/0016-7037(92)90173-G

Edem, D. E., Abba, M. K., Nourian, A., Babaie, M., and Naeem, Z. (2022). Experimental study on the interplay between different brine types/concentrations and CO2 injectivity for effective CO2 storage in deep saline aquifers. *Sustainability* 14, 986. doi:10.3390/su14020986

Frost, R. L., and Ruan, H. (2000). Dehydration and dehydroxylation of nontronites and ferruginous smectite. *Thermochim. Acta* 346, 63–72. doi:10.1016/S0040-6031(99)00366-4

Gadikota, G., Matter, J., Kelemen, P., and Park, A. A. (2014). Chemical and morphological changes during olivine carbonation for CO2 storage in the presence of NaCl and NaHCO3. *Phys. Chem. Chem. Phys.* 16, 4679. doi:10.1039/c3cp54903h

Goldberg, D. S., Takahashi, T., and Slagle, A. L. (2008). Carbon dioxide sequestration in deep-sea basalt. *PNAS* 105, 9920–9925. doi:10.1073/pnas.0804397105

Gudbrandsson, S., Wolff-Boenisch, D., Gislason, S. R., and Oelkers, E. H. (2011). An experimental study of crystalline basalt dissolution from 2≤pH≤11 and temperatures from 5 to 75°C. *Geochimica Cosmochimica Acta* 75, 5496–5509. doi:10.1016/j.gca.2011.06.035

Hassan, I., Antao, S. M., and Parise, J. B. (2006). Cancrinite: Crystal structure, phase transitions, and dehydration behavior with temperature. *Am. Mineralogist* 91, 1117–1124. doi:10.2138/am.2006.2013

Kelemen, P., Benson, S. M., Pilorgé, H., Psarras, P., and Wilcox, J. (2019). An overview of the status and challenges of CO2 storage in minerals and geological formations. *Front. Clim.* 1. doi:10.3389/fclim.2019.00009

Liu, C., Ma, H., and Gao, Y. (2019). Hydrothermal processing on potassic syenite powder: Zeolite synthesis and potassium release kinetics. *Adv. Powder Technol.* 30, 2483–2491. doi:10.1016/j.apt.2019.07.024

Marieni, C., Matter, J. M., and Teagle, D. A. H. (2020). Experimental study on mafic rock dissolution rates within CO2-seawater-rock systems. *Geochimica Cosmochimica Acta* 272, 259–275. doi:10.1016/j.gca.2020.01.004

Matter, J. M., Stute, M., Snaebjornsdottir, S. O., Oelkers, E. H., Gislason, S. R., Aradottir, E. S., et al. (2016). Rapid carbon mineralization for permanent disposal of anthropogenic carbon dioxide emissions. *Science* 352, 1312–1314. doi:10.1126/science.aad8132

National Academies of Sciences (2018). *Negative emissions technologies and reliable sequestration: A research agenda*. Washington, DC: National Academies Press. doi:10.17226/25259

Nesbitt, H. W., and Wilson, R. E. (1992). Recent chemical weathering of basalts. *Am. J. Sci.* 292, 740–777. doi:10.2475/ajs.292.10.740

Oelkers, E. H., Gislason, S. R., and Matter, J. (2008). Mineral carbonation of CO2. *Elements* 4, 333–337. doi:10.2113/gselements.4.5.333

Okoko, G. O., and Olaka, L. A. (2021). Can East african rift basalts sequester CO2? Case study of the Kenya rift. *Sci. Afr.* 13, e00924. doi:10.1016/j.sciaf.2021.e00924

Peter, A., Yang, D., Eshiet, K. I.-I. I., and Sheng, Y. (2022). A review of the studies on CO2–brine–rock interaction in geological storage process. *Geosciences* 12, 168. doi:10.3390/geosciences12040168

Rosenbauer, R. J., Thomas, B., Bischoff, J. L., and Palandri, J. (2012). Carbon sequestration via reaction with basaltic rocks: Geochemical modeling and experimental results. *Geochimica Cosmochimica Acta* 89, 116–133. doi:10.1016/j.gca.2012.04.042

Seo, S. M., Kim, D., Kim, D., Kim, J.-H., Lee, Y. J., Roh, K.-M., et al. (2018). A simple synthesis of nitrate cancrinite from natural bentonite. *J. Porous Mater* 25, 1561–1565. doi:10.1007/s10934-018-0569-4

Shibuya, T., Yoshizaki, M., Masaki, Y., Suzuki, K., Takai, K., and Russell, M. J. (2013). Reactions between basalt and CO_2-rich seawater at 250 and 350°C, 500bars: Implications for the CO_2 sequestration into the modern oceanic crust and the composition of hydrothermal vent fluid in the CO_2-rich early ocean. *Chem. Geol.* 359, 1–9. doi:10.1016/j.chemgeo.2013.08.044

Snæbjörnsdóttir, S. Ó., and Gislason, S. R. (2016). CO_2 storage potential of basaltic rocks offshore Iceland. *Energy Procedia* 86, 371–380. doi:10.1016/j.egypro.2016.01.038

Snæbjörnsdóttir, S. Ó., Sigfússon, B., Marieni, C., Goldberg, D., Gislason, S. R., and Oelkers, E. H. (2020). Carbon dioxide storage through mineral carbonation. *Nat. Rev. Earth Environ.* 1, 90–102. doi:10.1038/s43017-019-0011-8

Ueda, H., Shibuya, T., Sawaki, Y., Shozugawa, K., Makabe, A., and Takai, K. (2021). Chemical nature of hydrothermal fluids generated by serpentinization and carbonation of komatiite: Implications for H2-rich hydrothermal system and ocean chemistry in the early earth. *Geochem. Geophys. Geosystems* 22, e2021GC009827. doi:10.1029/2021GC009827

Voigt, M., Marieni, C., Baldermann, A., Galeczka, I. M., Wolff–Boenisch, D., Oelkers, E. H., et al. (2021). An experimental study of basalt–seawater–CO_2 interaction at 130 °C. *Geochimica Cosmochimica Acta* 308, 21–41. doi:10.1016/j.gca.2021.05.056

Wang, F., Dreisinger, D., Jarvis, M., and Hitchins, T. (2019). Kinetics and mechanism of mineral carbonation of olivine for CO_2 sequestration. *Miner. Eng.* 131, 185–197. doi:10.1016/j.mineng.2018.11.024

Wang, F., and Giammar, D. E. (2013). Forsterite dissolution in saline water at elevated temperature and high CO_2 pressure. *Environ. Sci. Technol.* 47, 168–173. doi:10.1021/es301231n

Wang, J., Watanabe, N., Inomoto, K., Kamitakahara, M., Nakamura, K., Komai, T., et al. (2021). Enhancement of aragonite mineralization with a chelating agent for CO_2 storage and utilization at low to moderate temperatures. *Sci. Rep.* 11, 13956. doi:10.1038/s41598-021-93550-9

Wang, J., Watanabe, N., Inomoto, K., Kamitakahara, M., Nakamura, K., Komai, T., et al. (2022). Sustainable process for enhanced CO_2 mineralization of calcium silicates using a recyclable chelating agent under alkaline conditions. *J. Environ. Chem. Eng.* 10, 107055. doi:10.1016/j.jece.2021.107055

Wang, J., Watanabe, N., Okamoto, A., Nakamura, K., and Komai, T. (2019b). Acceleration of hydrogen production during water-olivine-CO_2 reactions via high-temperature-facilitated Fe(II) release. *Int. J. Hydrogen Energy* 44, 11514–11524. doi:10.1016/j.ijhydene.2019.03.119

Wang, J., Watanabe, N., Okamoto, A., Nakamura, K., and Komai, T. (2019a). Enhanced hydrogen production with carbon storage by olivine alteration in CO_2-rich hydrothermal environments. *J. CO_2 Util.* 30, 205–213. doi:10.1016/j.jcou.2019.02.008

Wolff-Boenisch, D., and Galeczka, I. M. (2018). Flow-through reactor experiments on basalt-(sea)water-CO_2 reactions at 90°C and neutral pH. What happens to the basalt pore space under post-injection conditions? *Int. J. Greenh. Gas Control* 68, 176–190. doi:10.1016/j.ijggc.2017.11.013

Yamashita, S., Mukai, H., Tomioka, N., Kagi, H., and Suzuki, Y. (2019). Iron-rich smectite formation in subseafloor basaltic lava in aged oceanic crust. *Sci. Rep.* 9, 11306. doi:10.1038/s41598-019-47887-x

Zhao, Q., Liu, C., Jiang, M., Saxén, H., and Zevenhoven, R. (2015). Preparation of magnesium hydroxide from serpentinite by sulfuric acid leaching for CO_2 mineral carbonation. *Miner. Eng.* 79, 116–124. doi:10.1016/j.mineng.2015.06.002

Zhi, D., and Ying, H. (1993). A study on the dissolution kinetics of basalt-water interaction under different pH conditions I: Release of elements and pH neutralization effect. *Chin. J. Geochem.* 12, 183–191. doi:10.1007/BF02842199